Published-Ahead-of-Print on July 11, 2006 by Journal of Andrology

Tslc1 (Nectin-like molecule-2) is essential for spermatozoa motility and male fertility

Short title: Tslc1 regulates spermatozoa motility

Ezequiel I. Surace[1], Amy Strickland[2], Rex A. Hess[3], David H. Gutmann[1], and Cathy K. Naughton[2]

[1]Department of Neurology, [2]Department of Urologic Surgery, Washington University School of Medicine, St. Louis, MO, 63110, USA, and [3]Department of Veterinary Biosciences, University of Illinois at Urbana-Champaign, Urbana, IL, 61802, USA

Correspondence to: Cathy K. Naughton, MD, Department of Surgery, Division of Urology, Washington University School of Medicine, 1040 North Mason Road; Suite 122, St. Louis, MO 63141. Phone: 314-996-8071; FAX: 314-576-8880; E-mail: naughtonc@wustl.edu.

ABSTRACT

The nectin-like molecule-2 (TSLC1) is a cell-cell adhesion molecule expressed in testicular germ cells. To directly examine the role of Tslc1 in male fertility, we generated *Tslc1*+/- mice that have greater than 90% reduction in Tslc1 expression. *Tslc1*+/- males exhibit reduced fertility, and rarely transmitted the *Tslc1* mutant allele, whereas *Tslc1*+/- females were consistently able to transmit the mutant allele. Histologic and electron microscopic analyses of the testes in *Tslc1*+/- mice demonstrated disruption of the junctional scaffold between germ cells and Sertoli cells. Reduced Tslc1 expression had no effect on germ cell proliferation or apoptosis. While evidence of normal spermatozoal maturation was supported by Fluorescence Activated Cell Sorting (FACS) analysis, spermatozoa from *Tslc1*+/- mice demonstrated markedly reduced motility without compromised viability. Collectively, these results establish an essential role for Tslc1 in spermatozoal maturation and motility, distinct from other members of the nectin family.

Key words: spermatogenesis, spermiogenesis, testis, SynCAM1, IgSF4

INTRODUCTION

The Tumor Suppressor in Lung Cancer-1 (TSLC1 or nectin-like-2; necl-2) gene was originally identified as a candidate tumor suppressor on chromosome 11q23.2. TSLC1 expression is lost in multiple different human tumor types, including prostate cancer (Fukuhara et al, 2002), esophageal cancer (Ito et al, 2003), non-small cell lung cancer (Pletcher et al, 2001; Murakami, 2002; Mao et al, 2003), gastric cancer (Honda et al, 2002), breast cancer (Allinen et al, 2002), and meningioma (Surace et al, 2004). TSLC1 is a member of the nectin family of cell-cell adhesion proteins which are important for the organization of cell-cell junctions in epithelial cells (e.g., adherens and tight junctions), synaptic junctions in neurons (Biederer et al, 2002), and heterotypic junctions between germ cells and Sertoli cells in the testis (Wakayama et al, 2003). In this regard, TSLC1 is also named SynCAM1 based on its role in synaptic organization (Biederer et al, 2002) and IGSF4 based on its identification in male gonadal tissue (Wakayama et al, 2003).

TSLC1, like other members of the nectin superfamily, is composed of a large glycosylated extracellular region with three immunoglobulin (Ig)-like domains, a small transmembrane region, and a short cytoplasmic tail similar to glycophorin C and neurexin IV (Yageta et al, 2002). By analogy to nectin proteins, the first Ig-like loop is responsible for mediating interactions with nectin proteins on adjacent cells (trans-dimers), while the second Ig-like loop is responsible for nectin protein interactions within the same cell (cis-dimers) (Momose et al, 2002; Yasumi et al, 2003). The cytoplasmic tail of nectin proteins interacts with PDZ domain-containing proteins, like afadin, which may serve to link nectin proteins to the actin cytoskeleton (Miyoshi and Takai, 2005). In addition, nectin proteins have been shown to recruit

E-cadherin (Tachibana et al, 2000; Tanaka et al, 2003). As reported for other nectin-like proteins, TSLC1 does not bind afadin or recruit E-cadherin, but has been shown to interact with several other proteins, including Pals2 (Shingai et al, 2003), Protein 4.1B (Yageta et al, 2002), and MPP3 (Fukuhara et al, 2003), which are hypothesized to link TSLC1 to the actin cytoskeleton.

The role of nectin family proteins in the male gonad has been limited to studies of nectin-2 and nectin-3: nectin-2 is expressed exclusively in Sertoli cells, while nectin-3 expression is limited to spermatids (Ozaki-Kuroda et al, 2002). The heterotypic interaction between these two proteins is essential for normal spermatozoa maturation, such that nectin-2-deficient mice display loss of the junctional scaffold between Sertoli cells and spermatids, abnormal sperm morphogenesis, and infertility (Bouchard et al, 2000). Similar to nectin proteins, TSLC1 is robustly expressed in the male testis, where it is localized to germ cells (Wakayama et al, 2003). However, the function of TSLC1 in the male gonad is not known. In an effort to directly examine the role of TSLC1 in male fertility, we generated *Tslc1*+/- mice, and demonstrate that markedly reduced Tslc1 expression results in disrupted Sertoli cell-germ cell junctions, impaired spermatozoa motility, and reduced male fertility.

MATERIAL AND METHODS

Generation of Tslc1+/- mice

A total of five independent male chimeric *Tslc1*+/- mice were generated at the J. David Gladstone Institute (University of California, San Francisco) from the BayGenomics XI486 embryonic stem (ES) cell line (http://baygenomics.ucsf.edu) by blastocyst injection and transfer

into pseudopregnant female recipients using established protocols at the Gladstone Institute (Stryke et al, 2003; Austin et al, 2004). The XI486 ES cell line was generated using a trapping vector pGT1cd72 that contains an engrailed 2 gene intron upstream of a β-galactosidase and neomycin-resistance fusion protein (β-geo) gene. Two of the original five founder male mice (lines 1 and 4) had germline transmission of the *Tslc1* mutant allele, and both lines exhibited significantly reduced fertility. The most extensive analysis was conducted on line 4, and each experiment described in this report included specimens from at least nine individual *Tslc1*+/- mice. No *Tslc1*-/- mice were generated in this study. All studies were performed in strict compliance with federal guidelines and institutional policies at Washington University School of Medicine.

Reverse transcriptase-polymerase chain reaction (RT-PCR)

Total RNA was extracted from *Tslc1*+/- adult mouse brains using the Trizol reagent (Invitrogen), and first strand cDNA was synthesized from 5 µg total RNA using a reverse primer in the 5' end of the targeting vector (Trap-R: 5'- GACAGTATCGGCCTCAGGAAGATCG -3') in the presence of Superscript II reverse transcriptase (Invitrogen). After heat inactivation, the synthesized first strand cDNA was used as template in a PCR reaction using the Trap-R primer with either a forward primer in exon 3 (Ex3-F: 5' – GGGAGATACTTCTGCCAGCTCTACAC -3') or exon 4 (Ex4-F: 5'- GGCAGTTGAAGGGGAGGAGAT -3'). PCR amplification was performed in a thermocycler at 94°C for 1 minute, 55°C for 1 minute, 72°C for 2 minutes (29 cycles), and 72°C for 10 minutes. Five microliters of the PCR reaction were electrophoresed on 1% agarose gels, stained with ethidium bromide and visualized by UV transillumination.

β-galactosidase staining

Mouse brains were sectioned on a cryostat and 8 micron sections were incubated in X-gal (5-bromo-4-chloro-3-indolyl-ß-D-galactopyranoside) staining solution at 37°C for 24 hours, as previously reported (Bajenaru et al, 2002).

Western blot

Mouse tissues, including brain and testis as well as spermatozoa, were homogenized in lysis buffer (20mM Tris pH 7.5, 10mM EGTA, 40mM glycerol-2-phosphate, 1% NP40, 2.5mM $MgCl_2$, 2mM sodium orthovanadate), and total protein concentration was determined using the BCA kit (Pierce). Twenty-five micrograms of total protein were separated by SDS-polyacrylamide gel electrophoresis and transferred onto Immobilon membranes (Millipore) prior to blocking in 3% non-fat milk in PBS-Tween. The following primary antibodies were used: ES1 Tslc1 antibody (1:20,000 dilution; Surace et al, 2004), actin A2066 antibody (Sigma; 1:1000 dilution), tubulin T9026 antibody (Sigma; 1:20,000 dilution), nectin-2 rat monoclonal antibody (GeneTex, Inc.; 1:500 dilution), and β-galactosidase Z3781 antibody (Promega; 1:500 dilution). Western blots were developed using horseradish peroxidase-conjugated secondary antibodies (1:20,000) and ECL chemiluminescence (Amersham Biosciences) followed by exposure to radiographic film. Quantitation was performed by scanning densitometry using Gel Pro Analyzer software (Media Cybernetics, Silver Spring MD) and normalized to the tubulin expression in each sample.

Histology and fluorescence immunohistochemistry

Mouse testes were fixed in 4% paraformaldehyde or Bouin's solution overnight at 4°C, paraffin-embedded and serially cut on a microtome at 6 μm. For gross histological analysis, hematoxylin/eosin staining was performed. For fluorescence immunohistochemistry, sections were deparaffinized. Antigen retrieval was achieved by incubating the slides in 1mM EDTA and boiling for 30 minutes in a rice cooker. After blocking non-specific antibody binding sites in 5% horse serum/PBS, primary antibody (ES1, GCNA, and GATA4) was applied to the slides. The ES1 antibody was used at a 1:1,000 dilution, while antibodies against the GCNA (germ-cell nuclear antigen; gift from G. Enders, University of Kansas Medical Center, Kansas, USA; Enders and May, 1994) and the GATA4 (polyclonal H-112 antibody; Santa Cruz Biotechnology) were used at dilutions of 1:100 and 1:200, respectively. Nectin-2 (502-57) and nectin-3 (103-A1) rat monoclonal antibodies were used at 1:200 dilutions (GeneTex, Inc.). For GCNA, nectin-2, nectin-3 and ES1, Alexa 488 or Cy3-conjugated secondary antibodies (anti-rabbit for ES1 and anti-rat for GCNA, nectin-2, and nectin-3) were used. For GATA4, a biotinylated anti-goat secondary antibody followed by streptavidin-Cy2 (Jackson Immunoresearch) was used. Images were analyzed using a Nikon Eclipse TE300 fluorescence microscope equipped with a digital camera. All immunohistochemical studies were performed alongside negative controls (without primary antibody).

Evaluation of spermatozoa motility and viability

The entire epididymis from wild-type and *Tslc1*+/- mice was dissected away from the testis, cut into 3-4 pieces and incubated in 1ml M-16 media for 15 minutes at 37°C. Spermatozoa from the entire epididymis were released by passing the entire milliliter of suspension through a 70 μm mesh. The resulting suspension was collected in a 1.5 ml microcentrifuge tube, and

spermatozoa were collected by centrifugation at 3000 rpm for 5 minutes at 4°C. The supernatant was removed and the spermatozoa were resuspended in 1 ml of NIM solution (123 mM KCl, 2.6 mM NaCl, 7.8 mM NaH_2PO_4, 1.4 mM KH_2PO_4, 3 mM EDTA disodium salt; pH 7.2) and 1% polyvinyl alcohol. 15 µl of a 1:10 dilution of the spermatozoa suspension were counted on a hemacytometer, and >50 cells per mouse were scored as being motile or immotile. Viability was assessed by eosin-nigrosin staining of released epididymal spermatozoa (World Health Organization, 1999).

For detection of the targeted *Tslc1* allele in *Tslc1*+/- spermatozoa, DNA PCR was performed using primers contained within the β-geo cassette. Briefly, high molecular weight DNA was extracted from both wild-type and *Tslc1*+/- epididymal spermatozoa using standard methods. Approximately 100 ng of DNA were used in a PCR reaction containing a forward primer (8117; 5'-GAC ACC AGA CCA ACT GGT AAT GGT AGC GAC-3') and a reverse primer (8118; 5'-GCA TCG AGC TGG GTA ATA AGC GTT GGC AAT-3'). PCR amplification was performed in a thermocycler at 94°C for 3 minutes, 94°C for 1 minute, 62°C for 1 minute, 68°C for 3 minutes (38 cycles) and 68°C for 10 minutes. Five microliters of the PCR reaction were electrophoresed on 1% agarose gels, stained with ethidium bromide and visualized by UV transillumination.

TUNEL staining

Cell death was analyzed using the TUNEL assay (Roche Applied Bioscience) on 6 µm paraffin-embedded testis sections, representing 50 tubules per mouse. Specific signal was visualized by treatment with sheep peroxidase-conjugated anti-digoxigenin antibodies (1:1,000) followed by diaminobenzidine (DAB) development.

BrdU incorporation and staining

Mice were injected with 5-bromo-2-deoxyuridine (BrdU, Sigma) at a dose of 200 mg/kg two hours before euthanasia. Testes were removed and processed for immunohistochemistry using a mouse anti-BrdU antibody (Roche Boehringer Manheim, 1:200). Fifty tubules per mouse were analyzed.

Flow cytometric analysis of testis cells for DNA ploidy (FACS)

Testes were decapsulated and triturated into single cell suspensions in Hank's balanced salt solution containing 50 μg/ml propidium iodide (Sigma), 1mg/ml citric acid, and 0.3% NP40 for 30 minutes. Thirty thousand cells were analyzed for DNA content on a FACScan (Becton Dickinson) with FlowJo software (Tree Star, Version 4.3).

Transmission electron microscopy

Mice were perfused with PBS, then 4% paraformaldehyde. Testis tissue was fixed in 2.4% glutaraldehyde, 1% paraformaldehyde, 130mM cacodylate, and 1mM calcium chloride ($CaCl_2$) solution. Following fixation, the tissues were cut into approximately 1mm x 1mm pieces, which were rinsed in 0.1 M cacodylate buffer and post-fixed in 1% osmium tetroxide prior to embedding in Epon media. Ultrathin sections were visualized under a Morgagni transmission electron microscope as previously described (Nakai et al, 2002).

In vitro fertilization (IVF)

IVF was performed by the Mouse Genetics Core at the Washington University School of Medicine. Briefly, fresh epididymal spermatozoa were obtained as described above from *Tslc1*+/- mice and incubated in the presence of ova obtained from C57/Bl6 female mice. Four to six hours after incubation, ova were washed to remove excess spermatozoa, incubated overnight in HTF media (Quinn et al, 1985) and embryos transferred to pseudopregnant female mice.

Statistical analysis

Student's *t*-test was used for all analyses with significance set at $P < 0.05$.

RESULTS

Generation of Tslc1+/- mice

We employed insertional gene targeting to inactivate *Tslc1* in mice (BayGenomics; http://baygenomics.ucsf.edu). The embryonic stem cell line XI486 had the pGT1cd72 targeting vector inserted into intron 3 of the *Tslc1* gene located on mouse chromosome 9. This targeting vector was designed to contain a splice acceptor sequence, such that, upon transcription of the targeted *Tslc1* gene, the β-geo sequences would be spliced into the final *Tslc1* mRNA transcript (**Fig. 1A**). This insertion would result in loss of Tslc1 protein expression from that allele. To confirm the insertion site of the targeting vector, RT-PCR was performed on *Tslc1*+/- brain mRNA using a reverse primer in the 5' end of the vector (Trap-R) and a forward primer in the 3' end of exon 3 (Ex3F). Brain was initially chosen based on previously described high levels of Tslc1 expression in brain and meninges (Surace et al, 2004). A reaction using a forward primer 4 and the TRAP-R primer was included as a negative control (**Fig. 1B**). A PCR product was

obtained only with the Ex3F primer set, confirming that splicing occurred between the β-galactosidase gene in the vector and exon 3 in the *Tslc1* gene. Western blot analysis of total brain protein lysates from these *Tslc1*+/- mice showed >90% reduction in Tslc1 protein expression compared to normal brain by scanning densitometry (**Fig. 1C**). We expected that *Tslc1*+/- mice would exhibit a 50% reduction in Tslc1 protein expression; however, we consistently observed a greater than 90% reduction both in brain and testis (**Fig. 2B**).

One potential explanation for this dramatic reduction in Tslc1 expression is the generation of a dominant-interfering truncated Tslc1 fusion protein created by splicing of exons 1-3 to the β-galactosidase targeting vector sequence. To detect this potential Tslc1-βgal fusion protein, we performed Western immunoblotting using an antibody to β-galactosidase. We did not detect any such protein in brain, even with prolonged Western blot exposures (**Fig. 1D**). Similarly, X-gal staining of *Tslc1*+/- whole brain sections demonstrated very low levels of X-gal reactivity, even after 24 hours of development (**Fig. 1E**). As a positive control, we used a previously generated GFAP-Cre:IRES-LacZ mouse (Bajenaru et al, 2002), which demonstrates robust brain expression of the β-galactosidase protein both on Western blot (lane 1; **Fig. 1D**) and by X-gal staining (**Fig. 1E**).

Tslc1+/- male mice exhibit reduced fertility

While the *Tslc1*+/- mice did not have any obvious abnormal phenotype and did not exhibit reduced survival, we noticed that male *Tslc1*+/- mice consistently demonstrated reduced breeding. While some matings were able to produce a very small number of pups harboring the targeted *Tslc1* gene, eight of fourteen matings of proven fertile female mice with *Tslc1*+/- male mice did not result in the birth of any *Tslc1*+/- pups. Pregnancies were routinely verified by

plugs. In contrast, all female *Tslc1* +/- mice were able to breed normally and gave birth to pups harboring the mutant *Tslc1* gene in an expected Mendelian fashion (n>15 matings; 46 *Tslc1*+/- pups out of 71 total pups).

Tslc1 is normally expressed in testicular germ cells, but is nearly absent in Tslc1+/- testis

Tslc1 expression has been previously demonstrated in male germ cells of the mouse testis using both histological and electron microscopic methods (Wakayama et al, 2003). In contrast, other members of the nectin family (e.g., nectin-2 and nectin-3) show expression in Sertoli cells and not germ cells, or expression at different stages of germ cell maturation, suggesting that each of these molecules may be critical in certain gonadal cell types at specific times during germ cell development (Ozaki-Kuroda et al, 2002). To define the cell types expressing Tslc1 in the normal mouse testes, we performed co-localization studies with known cell-type specific markers (GCNA for germ cells and GATA4 for Sertoli cells) by fluorescence immunohistochemistry using a previously generated anti-Tslc1 antibody (Surace et al, 2004). We found that Tslc1 was expressed at the cytoplasmic membrane exclusively in germ cells (nuclear GCNA-immunoreactive spermatogonia and primary spermatocytes), but not in Sertoli cells with nuclear GATA4 immunostaining (**Fig. 2A**). Our results are similar to those obtained using a different Tslc1 antibody, in which cell surface expression of Tslc1 was found in intermediate/type B spermatogonia and spermatocytes (Wakayama et al, 2003). In addition, Tslc1 expression was also detected in elongating spermatids.

As observed in brains from *Tslc1*+/- mice, Tslc1 protein expression in the testes of heterozygous *Tslc1* males (n=9) also showed greater than >90% reduction compared to wild-type littermates (**Fig. 2B)**. To exclude the possibility that markedly reduced Tslc1 expression resulted

in alterations in nectin-2 and nectin-3 expression in the testis, we performed immunohistochemistry and Western blotting. We observed no changes in nectin-2 expression by Western blot in whole testis lysates from *Tslc1*+/- mice compared to wild-type controls (**Fig. 2C**). Similarly, no changes in the subcellular localization or expression of nectin-2 and nectin-3 by immunohistochemistry were seen in the testis from *Tslc1*+/- mice compared to controls (data not shown).

Tslc1+/- testis exhibits disrupted germ cell/Sertoli cell association

In order to assess the effect of reduced Tslc1 expression on cellular organization in the testis, we performed histological analysis using hematoxylin/eosin (H&E) staining and transmission electron microscopy. H&E staining revealed disruption of the basal compartment at the junction between germ cells and Sertoli cells in the *Tslc1+/-* mouse testis at various ages (3 weeks to 7 months; n=15 mice; **Fig. 2D**). Even in histologically normal appearing tubules, we detected disrupted architectural associations between germ cells and Sertoli cells by transmission electron microscopy (**Fig. 2E)**. In contrast to wild-type testes, *Tslc1*+/- mice exhibit a disorganization of the leptotene/pachytene spermatocyte region of the seminiferous epithelium. The junctions between Sertoli cells and these spermatocytes also appear to be disrupted, with the formation of extensive amounts of vacuolation and spaces in the base of the seminiferous tubules (denoted by the asterisks).

Tslc1+/- spermatozoa exhibit reduced cell motility

Given the gonadal histologic abnormalities observed in *Tslc1*+/- males, we sought to determine whether the disrupted Sertoli cell-germ cell associations result in abnormal

spermatozoa maturation. We first examined *Tslc1*+/- mice for changes in gonadal cell proliferation or apoptosis. No differences in cell proliferation or apoptosis as assessed by BrdU incorporation and TUNEL staining, respectively, were observed between wild-type and *Tslc1*+/- testes (data not shown). Next, we performed flow cytometric analyses of testis cells to detect defects in cell ploidy, and found no statistically significant differences in haploid (1N), diploid (2N) or tetraploid (4N) cell number between wild-type and *Tslc1*+/- mice (**Fig. 3A**). Moreover, light (n=15 mice) and electron (n=3 mice) microscopic analysis of spermatozoa collected from *Tslc1*+/- epididymii did not reveal any structural alterations (data not shown). Collectively, these results suggest that cell maturation, as measured by DNA content and morphology occurs normally in *Tslc1*+/- mice.

Since gametogenesis appeared normal, we next examined mature spermatozoa in the epididymis to detect possible abnormalities in the functional maturation of germ cells. In contrast to wild-type mouse sperm, we found a significant reduction in *Tslc1*+/- spermatozoa motility (n=15 mice; **Fig. 3B)**. In these experiments, we confirmed the presence of *Tslc1*-deficient spermatozoa in the samples by DNA PCR (**Fig. 3B,** inset panel) to exclude the possibility that no viable *Tslc1*-deficient spermatozoa were generated. Eosin-nigrosin staining showed that *Tslc1*-deficient spermatozoa showed no significant change in cell viability compared to wild-type spermatozoa (data not shown). To demonstrate that the reduced spermatozoal motility accounted for the reduced breeding observed in male *Tslc1*+/- mice, we performed *in vitro* fertilization (IVF). In this procedure, spermatozoa from *Tslc1*+/- mice were incubated in the presence of wild-type donor ova. Nineteen pups were generated by IVF, and all pups lacked the mutant *Tslc1* allele (data not shown).

Lastly, to determine whether Tslc1 is expressed in mature epididymal spermatozoa, Western blot analysis of wild-type mouse spermatozoa and whole testis was performed (**Fig. 3C**). We found that Tslc1 was not expressed in mature epididymal spermatozoa, suggesting that it most likely functions as an adhesion molecule important for defining the germ cell-Sertoli cell niche required for normal germ cell maturation.

DISCUSSION

The processes of spermatogenesis and spermiogenesis within the mammalian testis are highly dependent upon specific interactions between Sertoli cells and developing germ cells at critical times during gametogenesis. Sertoli cells maintain two types of specialized cell-cell junctions through structures termed ectoplasmic specializations. Basal ectoplasmic specializations form between Sertoli cells near the base of the epithelium, while apical ectoplasmic specializations form between Sertoli cells and the heads of elongated spermatids (Russell, 1997; Vogl et al, 1989; Vogl et al, 2000). Apical ectoplasmic specializations are not only responsible for linking the spermatid to the Sertoli cell, but also for the translocation of spermatids through the seminiferous epithelium and their timely release into the lumen.

It is not known what specific molecular cues emanate from Sertoli cells to dictate normal germ cell maturation. Recent studies have implicated nectin molecules as important proteins that mediate cell-cell interactions which result in the generation of specific intracellular signals that drive normal male gametogenesis. Examination of nectin-2 and nectin-3 expression and function in the male gonad demonstrate that these molecules are critical not only for the proper maintenance of normal cell architecture within the seminiferous tubule, but also for the

formation of mature spermatozoa (Bouchard et al, 2000; Ozaki-Kuroda et al, 2002; Mueller et al, 2003). In this regard, male mice lacking either nectin-2 or nectin-3 are infertile (Bouchard et al, 2000; Ozaki-Kuroda et al, 2002; Mueller et al, 2003; Inagaki et al, 2005; Miyoshi and Takai, 2005).

Immunohistochemical analyses have shown that each nectin protein has a distinct pattern of expression: Sertoli cells express nectin-2, but lack nectin-3 and Tslc1 expression (Ozaki-Kuroda et al, 2002; Wakayama et al, 2003). Whereas Tslc1 is expressed in spermatogonia, spermatocytes, and spermatids, nectin-3 expression is found only in spermatids (Guttman et al, 2004). This temporal pattern of Tslc1 and nectin-3 expression suggests that their functions are non-redundant, and that nectin-3 cannot compensate for Tslc1 loss during early spermatogenesis. Moreover, we performed immunostaining and Western blot analysis of nectin-2 and -3 in *Tslc1* +/- testis and found no differences in their overall expression patterns or cellular localization compared to wild-type controls. This result further supports the notion that other nectins expressed in the male gonad do not compensate for Tslc1 loss.

While no detailed reports exist describing the structural or functional abnormalities in nectin-3 knockout mice, nectin-2-deficient mice produce severely deformed spermatozoa with malformations of the head and midpiece, but no defects in either sperm viability or motility (Mueller et al, 2003). The infertility phenotype of mice lacking nectin-2 likely reflects defects in spermatozoa-zona binding and sperm-oocyte fusion. Moreover, the Sertoli-spermatid junctions in these nectin-2-deficient mice are virtually devoid of the actin-binding protein, espin. The defect in spermatogenesis in *Tslc1*+/- mice is distinct from that observed in nectin-2-deficient mice, suggesting a unique function for Tslc1. In contrast to nectin-2-deficient mice, *Tslc1*+/- spermatozoa were morphologically normal, and demonstrated disrupted interactions with Sertoli

cells at an early stage in sperm maturation. Since Tslc1 is only expressed in germ cells, and not in mature epididymal spermatozoa, binding between Tslc1 on germ cells and cell surface proteins expressed on Sertoli cells imparts a novel signal important for male germ cell maturation. We hypothesize that Tslc1 is critical for specifying interactions between germ cells and Sertoli cells during early testicular germ cell maturation. Impairment of this interaction in *Tslc1*+/- mice results in incomplete spermatogonia maturation, abnormal spermatozoa motility, and reduced male fertility.

In this report, we show that Tslc1 (nectin-like 2 molecule) has a unique role in the maintenance of the Sertoli cell/germ cell association, which is critical for the acquisition of the motile sperm phenotype. These results extend our understanding of the role of the nectin family of proteins in specifying male germ cell maturation and demonstrate that each nectin protein functions in a non-redundant fashion at a temporally distinct phase of germ cell development. Additional studies on the role of TSLC1 in gonadal maturation relevant to the acquisition of a motile sperm phenotype may provide important insights into the molecular pathogenesis of male-factor fertility in men with isolated asthenospermia.

Acknowledgments. We thank Dr. Stephen G. Young (J. David Gladstone Institute; University of California, San Francisco) for generating the *Tslc1*+/- mice. We also thank Mr. Scott Bahr for technical assistance. This work was supported by funding from the Department of Defense (DAMD-17-04-0266; to DHG).

REFERENCES

Allinen M, Peri L, Kujala S, Lahti-Domenici J, Outila K, Karppinen SM, Launonen V, Winqvist R. Analysis of 11q21-24 loss of heterozygosity candidate target genes in breast cancer: indications of TSLC1 promoter hypermethylation. Genes Chromosomes Cancer. 2002;34:384-389.

Austin CP, Battey JF, Bradley A, Bucan M, Capecchi M, Collins FS, Dove WF, Duyk G, Dymecki S, Eppig JT, Grieder FB, Heintz N, Hicks G, Insel TR, Joyner A, Koller BH, Lloyd KC, Magnuson T, Moore MW, Nagy A, Pollock JD, Roses AD, Sands AT, Seed B, Skarnes WC, Snoddy J, Soriano P, Stewart DJ, Stewart F, Stillman B, Varmus H, Varticovski L, Verma IM, Vogt TF, von Melchner H, Witkowski J, Woychik RP, Wurst W, Yancopoulos GD, Young SG, Zambrowicz B. The knockout mouse project. Nat. Genet. 2004;36:921-924.

Bajenaru ML, Zhu Y, Hedrick NM, Donahoe J, Parada LF, Gutmann DH. Astrocyte-specific inactivation of the neurofibromatosis 1 gene (NF1) is insufficient for astrocytoma formation, Mol. Cell. Biol. 2002;22:5100-5113.

Biederer T, Sara Y, Mozhayeva M, Atasoy D, Liu X, Kavalali ET, Sudhof TC. SynCAM, a synaptic adhesion molecule that drives synapse assembly. Science. 2002;297:1525-1531.

Bouchard MJ, Dong Y, McDermott BM, Lam DH, Brown KR, Shelanski M, Bellve AR, Racaniello VR. Defects in nuclear and cytoskeletal morphology and mitochondrial localization in spermatozoa of mice lacking nectin-2, a component of cell-cell adherens junctions. Mol. Cell. Biol. 2000;20:2865-2873.

Enders GC, May, JJ. Developmentally regulated expression of a mouse germ cell nuclear antigen examined from embryonic day 11 to adult in male and female mice. Dev. Biol. 1994;163:331-340.

Fukuhara H, Kuramochi M, Fukami T, Kasahara K, Furuhata M, Nobukuni T, Maruyama T, Isogai K, Sekiya T, Shuin T, Kitamura T, Reeves RH, Murakami Y. Promoter methylation of TSLC1 and tumor suppression by its gene product in human prostate cancer. Jpn. J. Cancer Res. 2002;93:605-609.

Fukuhara H, Masuda M, Yageta M, Fukami T, Kuramochi M, Maruyama T, Kitamura T, Murakami Y. Association of a lung tumor suppressor TSLC1 with MPP3, a human homologue of Drosophila tumor suppressor Dlg. Oncogene 2003;22:6160-6165.

Guttman JA, Takai Y, Vogl AW. Evidence that tubulobulbar complexes in the seminiferous epithelium are involved with internalization of adhesion junctions. Biol. Reprod. 2004;71:548-559.

Honda T, Tamura G, Waki T, Jin Z, Sato K, Motoyama T, Kawata S, Kimura W, Nishizuka S, Murakami Y. Hypermethylation of the TSLC1 gene promoter in primary gastric cancers and gastric cancer cell lines. Jpn. J. Cancer Res. 2002;93:857-860.

Inagaki M, Irie K, Ishizaki H, Tanaka-Okamoto M, Morimoto K, Inoue E, Ohtsuka T, Miyoshi J, Takai Y. Roles of cell-adhesion molecules nectin 1 and nectin 3 in ciliary body development. Development. 2005;132:1525-1537.

Ito T, Shimada Y, Hashimoto Y, Kaganoi J, Kan T, Watanabe G, Murakami Y, Imamura M. Involvement of TSLC1 in progression of esophageal squamous cell carcinoma. Cancer Res. 2003;63:6320-6326.

Mao XE, Seidlitz E, Ghosh K, Murakami Y, Ghosh HP. The cytoplasmic domain is critical to the tumor suppressor activity of TSLC1 in non-small cell lung cancer. Cancer Res. 2003;63:7979-7985.

Miyoshi J, Takai Y. Molecular perspective on tight-junction assembly and epithelial polarity. Adv. Drug Deliv. Rev. 2005;57:815-855.

Momose Y, Honda T, Inagaki M, Shimizu K, Irie K, Nakanishi H, Takai Y. Role of the second immunoglobulin-like loop of nectin in cell-cell adhesion. Biochem. Biophys. Res. Commun. 2002;293:45-49.

Mueller S, Rosenquist TA, Takai Y, Bronson RA, Wimmer E. Loss of nectin-2 at Sertoli-spermatid junctions leads to male infertility and correlates with severe spermatozoan head and midpiece malformation, impaired binding to the zona pellucida, and oocyte penetration. Biol. Reprod. 2003;69:1330-1340.

Murakami Y. Functional cloning of a tumor suppressor gene, TSLC1, in human non-small cell lung cancer. Oncogene. 2002;21:6936-6948.

Nakai M, Miller MG, Carnes K, Hess RA. Stage-specific effects of the fungicide carbendazim on Sertoli cell microtubules in rat testis. Tissue Cell. 2002;34:73-80.

Ozaki-Kuroda K, Nakanishi H, Ohta H, Tanaka H, Kurihara H, Mueller S, Irie K, Ikeda W, Sakai T, Wimmer E, Nishimune Y, Takai Y. Nectin couples cell-cell adhesion and the actin scaffold at heterotypic testicular junctions. Curr. Biol. 2002;12:1145-1150.

Pletcher MT, Nobukuni T, Fukuhara H, Kuramochi M, Maruyama T, Sekiya T, Sussan T, Isomura M, Murakami Y, Reeves RH. Identification of tumor suppressor candidate genes by physical and sequence mapping of the TSLC1 region of human chromosome 11q23. Gene. 2001;273:181-189.

Quinn P, Kerin JF, Warnes GM. Improved pregnancy rate in human in vitro fertilization with the use of a medium based on the composition of human tubal fluid. Fertil. Steril. 1985;44:493-498.

Russell L. Observations on rat Sertoli ectoplasmic ('junctional') specializations in their association with germ cells of the rat testis. Tissue Cell. 1997;9:475-498.

Shingai T, Ikeda W, Kakunaga S, Morimoto K, Takekuni K, Itoh S, Satoh K, Takeuchi M, Imai T, Monden M, Takai Y. Implications of nectin-like molecule-2/IGSF4/RA175/SgIGSF/TSLC1/SynCAM1 in cell-cell adhesion and transmembrane protein localization in epithelial cells. J. Biol. Chem. 2003;278:35421-35427.

Stryke D, Kawamoto M, Huang CC, Johns SJ, King LA, Harper CA, Meng EC, Lee RE, Yee A, L'Italien L, Chuang P-T, Young SG, Skarnes WC, Babbitt PC, Ferrin TE. BayGenomics: a resource of insertion mutations in mouse embryonic stem cells. Nucleic Acids Res. 2003;31:278-281.

Surace EI, Lusis E, Murakami Y, Scheithauer BW, Perry A, Gutmann DH. Loss of tumor suppressor in lung cancer-1 (TSLC1) expression in meningioma correlates with increased malignancy grade and reduced patient survival. J. Neuropathol. Exp. Neurol. 2004;63:1015-1027

Tachibana K, Nakanishi H, Mandai K, Ozaki K, Ikeda W, Yamamoto Y, Nagafuchi A, Tsukita S, Takai Y. Two cell adhesion molecules, nectin and cadherin, interact through their cytoplasmic domain-associated proteins. J. Cell. Biol. 2000;150:1161-1176.

Tanaka Y, Nakanishi H, Kakunaga S, Okabe N, Kawakatsu T, Shimizu K, Takai Y. Role of nectin in formation of E-cadherin-based adherens junctions in keratinocytes: analysis with the N-cadherin dominant negative mutant. Mol. Biol. Cell. 2003;14:1597-1609.

Vogl AW. Distribution and function of organized concentrations of actin filaments in mammalian spermatogenic cells and Sertoli cells. Int. Rev. Cytol. 1989;119:1-56.

Vogl AW, Pfeiffer DC, Mulholland D, Kimel G, Guttman J. Unique and multifunctional adhesion junctions in the testis: ectoplasmic specializations. Arch. Histol. Cytol. 2000;63:1-15.

Wakayama T, Koami H, Ariga H, Kobayashi D, Sai Y, Tsuji A, Yamamoto M, Iseki S. Expression and functional characterization of the adhesion molecule spermatogenic immunoglobulin superfamily in the mouse testis. Biol. Reprod. 2003;68:1755-1763.

World Health Organization. Laboratory Manual for the Examination of Human Semen and Sperm-Cervical Mucus Interaction. Cambridge:Cambridge University Press; 1999.

Yageta M, Kuramochi M, Masuda M, Fukami T, Fukuhara H, Maruyama T, Shibuya M, Murakami Y. Direct association of TSLC1 and DAL-1, two distinct tumor suppressor proteins in lung cancer. Cancer Res. 2002;62:5129-5133.

Yasumi M, Shimizu K, Honda T, Takeuchi M, Takai Y. Role of each immunoglobulin-like loop of nectin for its cell-cell adhesion activity. Biochem. Biophys. Res. Commun. 2003;302:61-66.

FIGURE LEGENDS

Fig. 1. ES Cell line XI486 from BayGenomics Gene Trap library targets the Mouse *Tslc1* gene. **A)** Schematic diagram of part of the genomic sequence of *Tslc1* on chromosome 9 (top panel). The pGTcd72 targeting vector containing a β-geo gene (β –galactosidase/neomycin-resistance) was inserted in intron 3 (middle panel). After transcription, the targeting vector is spliced into the mRNA downstream of *Tslc1* exon 3 generating an altered transcript (bottom panel). **B)** RT-PCR from *Tslc1*+/- mouse brain mRNA was performed using a reverse primer in the 5' end of the targeting vector and a forward primer in the 3' end of exon 3 (Ex3F). As a control, a forward primer in exon 4 (Ex4F) was used with the same reverse primer in the targeting vector. A product was detected only when the Ex3F primer set was used (arrow), confirming the vector insertion site reported by BayGenomics. The first lane contains the molecular size markers (L). **C)** Western blot analysis shows reduction in Tslc1 expression in brains from adult *Tslc1*+/- mice compared to wild-type (WT) mice using a previously generated polyclonal antibody against Tslc1 (ES1). Tubulin is included as a loading control. **D)** In order to detect the presence of a Tslc1 fusion protein, Western blot analysis using β-galactosidase and Tslc1 antibodies was performed. No truncated fusion peptide was detected. GFAP-Cre:IRES-LacZ mouse brain lysates were used as a positive control. **E)** β-galactosidase staining (X-gal cytochemistry) showed no β-galactosidase activity in *Tslc1*+/- mouse brain. GFAP-Cre:IRES-LacZ mouse brain was used as a positive control, while a wild-type (WT) mouse brain was included as a negative control for X-gal staining.

Fig. 2. Analysis of *Tslc1*+/- seminiferous tubules shows disrupted germ cell /Sertoli cell association. A) Left panel, double-labeled fluorescence immunohistochemistry on wild-type mouse testis sections shows that Tslc1 (red) is predominantly expressed in germ cells expressing the germ cell nuclear antigen, GCNA (green). **Right panel**, staining with an antibody against the Sertoli cell marker GATA4 (green) shows that Sertoli cells do not express Tslc1 (red). Photomicrographs were taken at 200X. **B)** Western blot analysis using the ES1 antibody shows a marked reduction in Tslc1 expression in testes of *Tslc1*+/- mice compared to wild-type (WT) controls. Tubulin is used as a loading control. **C)** Western blot analysis of nectin-2 expression in five representative *Tslc1*+/- testis lysates compared to wild-type (WT) testis. Actin was used as an internal control for equal protein loading. No changes in nectin-2 expression were noted. **D)** Hematoxylin and eosin stained testicular sections show a ring-like pattern suggestive of basal compartment disruption. Photomicrographs were taken at 200X. **E)** Transmission electron microscopy confirmed the presence of abnormal junctions between germ cells and Sertoli cells. Asterisks denote examples of disrupted Sertoli cell/germ cell junctions. The specific cell types in the photomicrograph include P (pachytene spermatocyte), L (leptotene spermatocyte), 8 (step 8 spermatid), Pre (preleptotene spermatocyte), and SC (Sertoli cell). Photomicrographs were taken at 1600X.

Fig. 3. *Tslc1*+/- testis exhibits normal cell maturation but epididymal spermatozoa have reduced motility. A) Flow cytometric analysis showed no statistically significant differences in cell ploidy (1N, 2N and 4N cell populations) between wild-type and *Tslc1*+/- mice. Mean +/- SD are shown. N.S. = not significant (Student's *t*-test). **B)** Epididymal spermatozoa from wild-type and *Tslc1*+/- mice were obtained, and motile cells were counted on a hemacytometer. *Tslc1*+/-

spermatozoa cells exhibited a marked reduction in motility when compared to wild-type cells ($P<0.001$). Mean +/- SD are shown. Inset panel: DNA was extracted from both wild-type (WT) and *Tslc1*+/- spermatozoa and used as template for PCR with primers within the β-geo gene. Results show the presence of Tslc1-deficient spermatozoa. **C)** Wild-type epididymal spermatozoa lack Tslc1 expression (top panel). Tubulin was used as a loading control (bottom panel).

Summary Statement. The nectin-like molecule-2 is essential for mouse spermatozoa motility and male fertility.

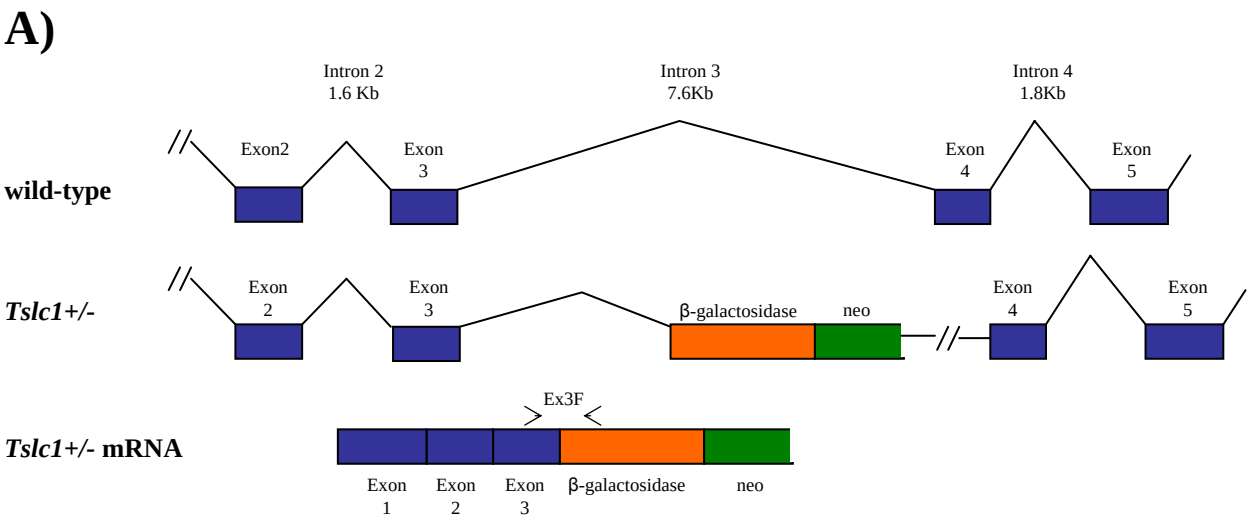
A)
Intron 2
1.6 Kb
Intron 3
7.6Kb
Intron 4
1.8Kb
wild-type
Exon2
Exon
3
Exon
4
Exon
5
Tslc1+/-
Exon
2
Exon
3
β-galactosidase
neo
Exon
4
Exon
5
Tslc1+/- mRNA
Ex3F
Exon
1
Exon
2
Exon
3
β-galactosidase
neo

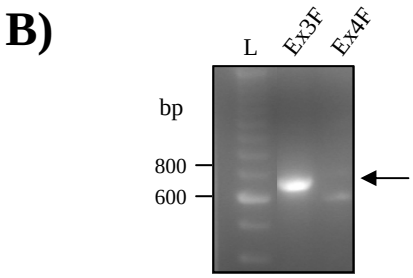
B)
L
Ex3F
Ex4F
bp
800
600

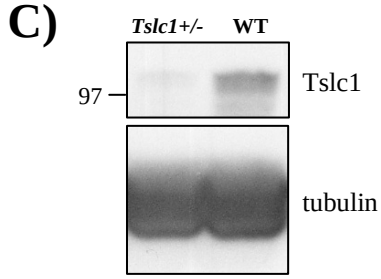
C)
Tslc1+/-
WT
97
Tslc1
tubulin

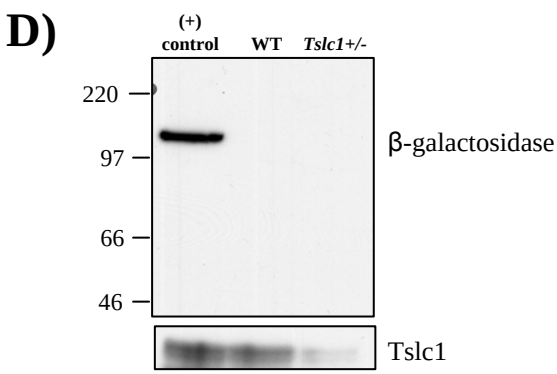
D)
(+)
control
WT
Tslc1+/-
220
97
66
46
β-galactosidase
Tslc1

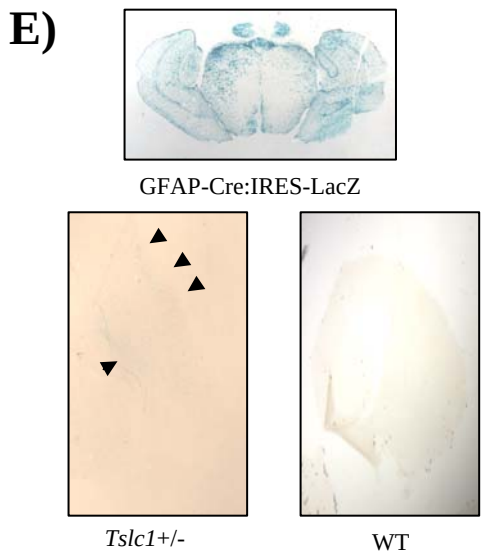
E)
GFAP-Cre:IRES-LacZ
Tslc1+/-
WT

A)

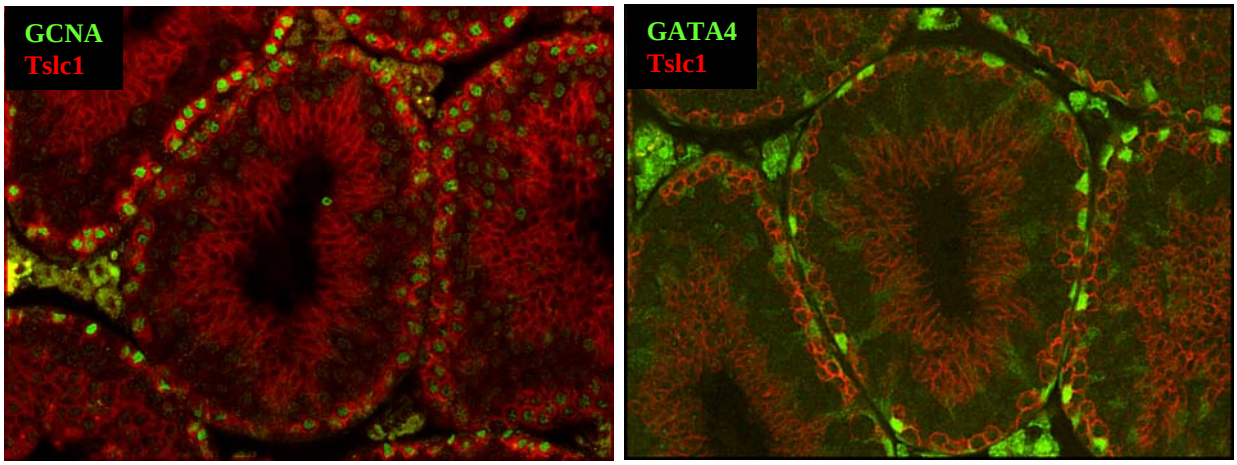
GCNA
Tslc1
GATA4
Tslc1

B)

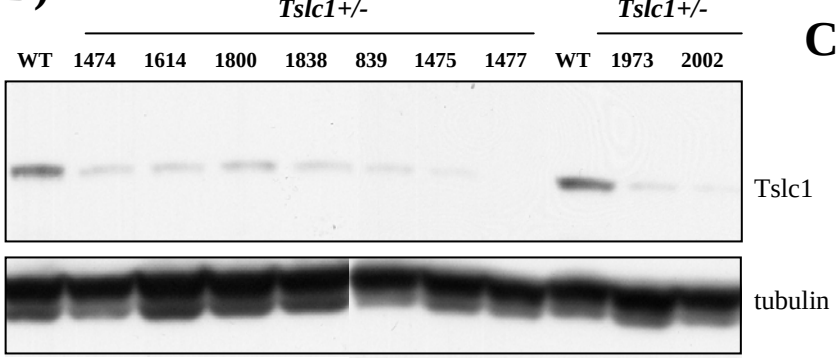
Tslc1+/-
Tslc1+/-
WT
1474
1614
1800
1838
839
1475
1477
WT
1973
2002
Tslc1
tubulin

C)

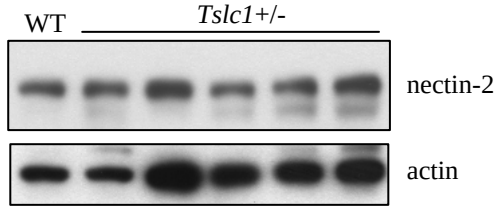
WT
Tslc1+/-
nectin-2
actin

D)

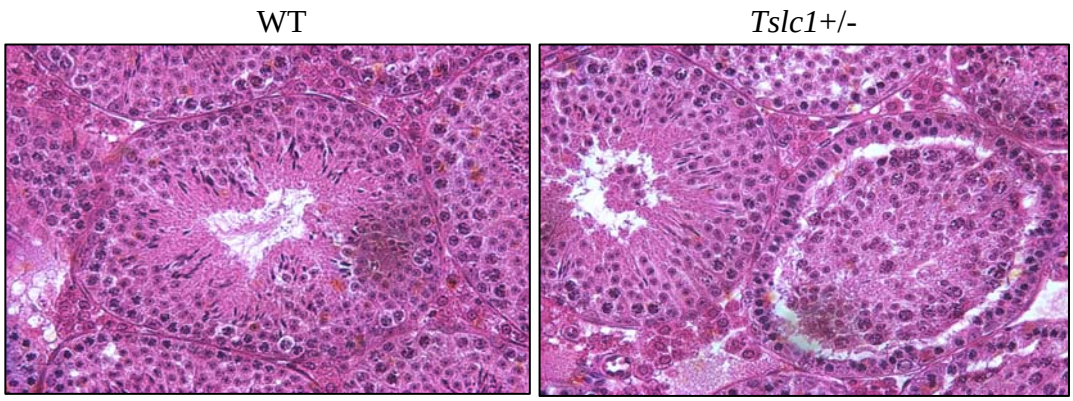
WT
Tslc1+/-

E)

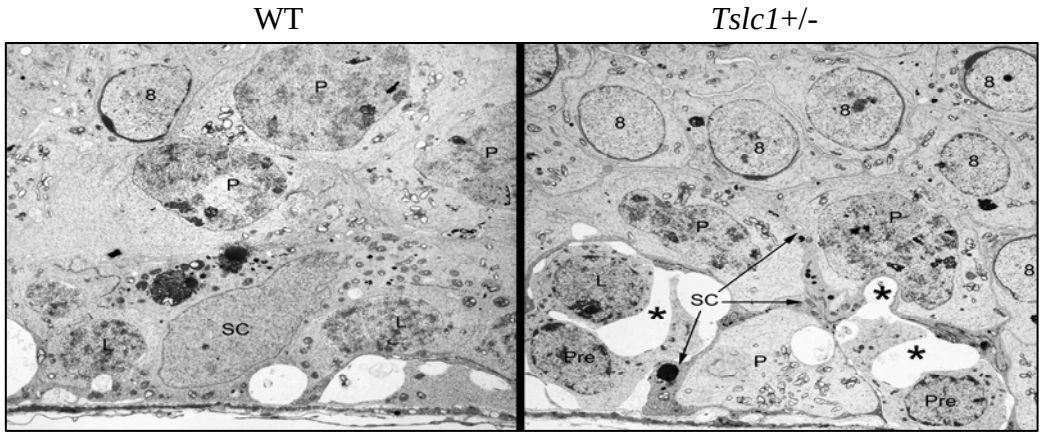
WT
Tslc1+/-
8
P
SC
L
Pre
*

A)

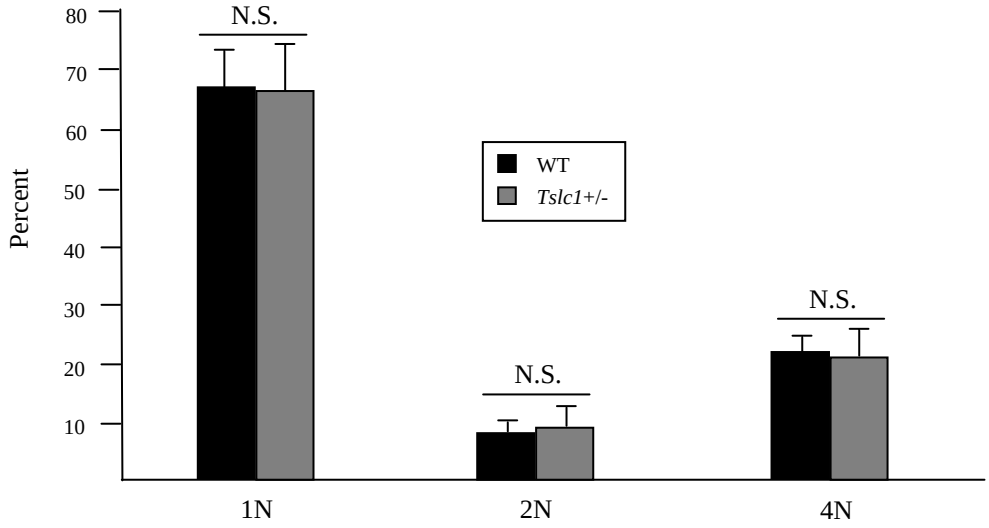
Percent
80
70
60
50
40
30
20
10
N.S.
N.S.
N.S.
WT
Tslc1+/-
1N
2N
4N

B)

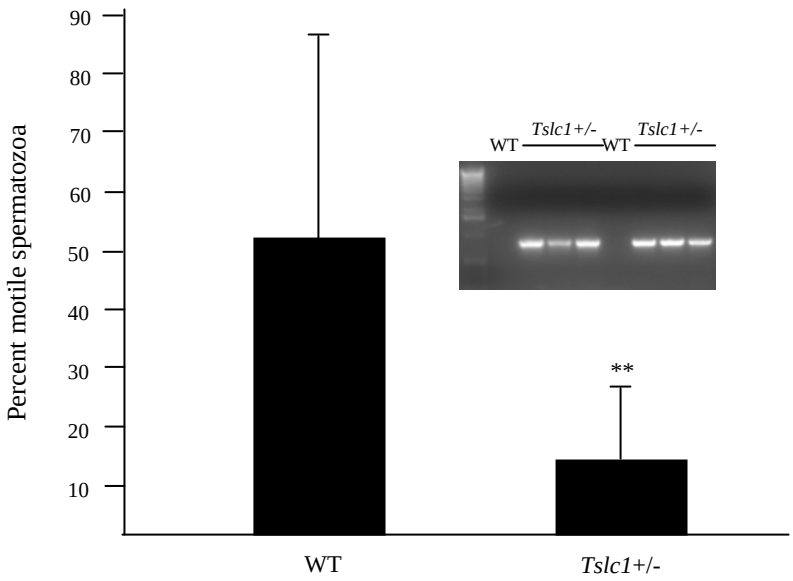
Percent motile spermatozoa
90
80
70
60
50
40
30
20
10
WT
Tslc1+/-
WT
Tslc1+/-
WT
Tslc1+/-
**

C)

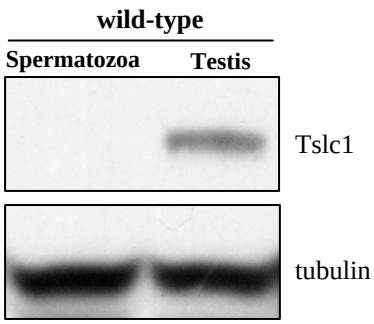
wild-type
Spermatozoa
Testis
Tslc1
tubulin